


Analytic Analysis for Dynamic System Frequency in Power Systems Under Uncertain Variability

Hongyu Li , *Student Member, IEEE*, Ping Ju , *Senior Member, IEEE*, Chun Gan , *Member, IEEE*, Shutang You , *Student Member, IEEE*, Feng Wu , and Yilu Liu , *Fellow, IEEE*

Abstract—In this paper, a new systematic method is proposed to analyze the system frequency in power systems under uncertain variability (UV). UV gradually increases in power systems, which originates from the renewable energy generation, random loads, frequency measurement, and communication channels, exerting noteworthy impacts on dynamic system frequency. The UV is modeled as a stochastic process in this paper. Then, the stochastic differential equations are used to describe the dynamic system frequency response (SFR) of a power system under UV, which is based on the SFR model. To assess system frequency dynamics under UV, an index of intra-range probability is put forward. Based on stochastic analysis theory, an analytic method is proposed to analyze the system frequency under UV, by which the intra-range probability can be analytically solved. Compared with Monte Carlo simulation in a typical SFR case and the Iceland electricity transmission network, the proposed method shows almost the same results using much less computation resource. Finally, insights for improving the SFR under UV are provided. The proposed method can be used to quickly verify whether the system frequency could withstand the UV and stay in the security range.

Index Terms—Stochastic differential equations, system frequency response (SFR), stochastic process, intra-range probability, Monte Carlo simulation.

I. INTRODUCTION

THE considerable attention has been paid to the uncertainty in power systems [1]–[8]. Uncertain variability (UV) always exists, but it was considered small in conventional power

systems. However, with the increasing penetration of plug-in electric vehicles [9], [10] and intermittent renewable energy [11]–[13], UV in power systems becomes much larger in recent years. Power systems are suffering from the ever-growing UV. As a key factor of power systems, the system frequency is of concern when UV is introduced. In [14], the authors are commended for proposing a novel framework to assess the impacts of the UV from load variations, renewable based generation, and noise in communication channels on the automatic generation control system. In [15], a novel stochastic model is proposed to analyze system frequency variations by considering the dynamic coupling of the transmission system, electricity market, and microgrids. In this paper, the main work is focused on the analytic analysis for dynamic system frequency in power systems under UV.

The system frequency response (SFR) model is widely used to analyze the system frequency, which is initially proposed in [16] to estimate the system frequency behavior of a large power system or the islanded portion under disturbances. In [17], an improved average SFR model is proposed to evaluate the contribution of inertial and droop responses from a wind farm for the short-term frequency regulation. The role of electric vehicles contributing to the primary frequency response is investigated in [18], by using the SFR model. In [19], the stochastic decentralized active demand response system is applied to design the frequency controller, based on the SFR model. Using the SFR model, intelligent regional demand response is proposed to cooperate in controlling the system frequency of a multi-area power system [20]. In [21], a new SFR model incorporating an under-frequency load-shedding scheme is proposed, in which closed-form expressions of the load-frequency response is derived. For power systems including conventional synchronous machines and modern WTGs, a novel method using the SFR model to calculate the power system frequency is presented in [22]. In [23], a methodology based on the SFR model is proposed to analyze the system frequency dynamics of large-scale power systems with the high-level wind energy penetration. In [24], the effect of frequency-sensitive load on system frequency is investigated by using the typical SFR model. In [25], an analytical adaptive load shedding scheme against deterministic severe combinational disturbances is proposed based on the SFR mode. A novel load-damping characteristic control method in an isolated power system with industrial voltage-sensitive load is proposed in [26] by using the SFR model. In [27], a convenient way is provided to unify the model for Type 3 wind turbines

Manuscript received November 22, 2017; revised March 29, 2018; accepted September 16, 2018. Date of publication October 1, 2018; date of current version February 18, 2019. This work was supported in part by the “111” project of “Renewable Energy and Smart Grid” under Grant B14022, and in part by the National Natural Science Foundation of China under Grants 51422701, 51707056, and 51837004. Paper no. TPWRS-01764-2017. (*Corresponding author: Ping Ju.*)

H. Li is with the College of Energy and Electrical Engineering, Hohai University, Nanjing 211100 China, and also with the Department of Electrical Engineering and Computer Science, University of Tennessee, Knoxville, TN 37996 USA (e-mail: hongyu.li.1990@gmail.com).

P. Ju is with the College of Energy and Electrical Engineering, Hohai University, Nanjing 211100 China, and also with Zhejiang University, Hangzhou 310027, China (e-mail: pju@hhu.edu.cn).

C. Gan is with the School of Electrical and Electronic Engineering, Huazhong University of Science and Technology, Wuhan 430074, China (e-mail: chungan@hust.edu.cn).

S. You and Y. Liu are with the Department of Electrical Engineering and Computer Science, University of Tennessee, Knoxville, TN 37996 USA (e-mail: syou3@vols.utk.edu; liu@utk.edu).

F. Wu is with the College of Energy and Electrical Engineering, Hohai University, Nanjing 211100, China (e-mail: wufeng@hhu.edu.cn).

Color versions of one or more of the figures in this paper are available online at <http://ieeexplore.ieee.org>.

Digital Object Identifier 10.1109/TPWRS.2018.2873410

with a typical SFR model of synchronous generators to construct frequency dynamics analysis for large-scale power systems. In [28], the SFR model is utilized to integrate renewable resources into power systems without violating system frequency limits, in which the loss of the largest unit for the 118-bus system is simulated by a 10% sudden increase in the load. In [29], the impact of frequency sensitive loads on system frequency is analyzed when the wind farm is integrated with the conventional power system, in which the deterministic perturbation trajectories are used for the load and wind speed. From the above references, it can be found that the SFR model has high accuracy to analyze the system frequency. However, the UV was seldom considered, such as the random fluctuations from the generation and loads, stochastic errors of measurement, and noise in communication channels.

Based on the theory of stochastic calculus, power systems under UV can be modeled by a set of stochastic differential equations (SDEs) [30]–[41]. In [42], a systematic method is proposed to model stochastic power systems using stochastic differential-algebraic equations. In [43], power systems influenced by stochastic perturbations in load and variable renewable generation are modeled by stochastic differential-algebraic equations. Specifically, the stochastic excitation is adopted to describe the mechanical power input of an asynchronous wind turbine, and then a power system under stochastic excitation is modeled as SDEs [44]. In [45], a single-machine infinite-bus (SMIB) system is modeled as a stochastic model based on SDEs, and the stability of this stochastic system is assessed. The stochastic perturbations in transmission lines and system loads are considered in [46], and then the power system under these perturbations is described by a set of SDEs. In [47], an SDE-based model which includes uncertainties in the system load at the wind generator bus is presented. In [48], a stochastic model based on SDEs is employed to describe power systems with variable wind power. By utilizing SDEs, continuous wind speed models are proposed in [49]. In this paper, SDEs are adopted to describe power systems under UV.

In recent years, the research on analyzing power systems under UV has attracted much attention. However, several issues have not been addressed yet: (1) the impacts of UV on the system frequency are seldom investigated; (2) in the methods to analyze the impacts of UV on the system frequency, analytic methods that can provide sufficient accuracy with high efficiency still has not been presented; (3) the analysis index that meet engineer's requirements about the system frequency are not proposed, such as the probability of system frequency being in the security range.

To deal with the issues mentioned above, this paper proposes a systemic analytic method for analyzing the system frequency under UV. To describe the UV, stochastic processes are adopted. Furthermore, the SFR model incorporating UV is formulated as SDEs. The intra-range probability is presented to assess the system frequency under UV. Based on stochastic theory, a systemic analytic method is put forward to analytically calculate the intra-range probability. Compared with Monte Carlo simulation, the proposed analytic method has two significant advantages: first,

the higher efficiency with similar accuracy; second, a clearer impact mechanism of UV on system frequency. Finally, impacts of SFR model's parameters on the system frequency under UV is offered, providing insights for improving SFR under UV.

Compared with previous studies, there are five main contributions in this paper, which are clarified point by point and compared with existed papers in the following: (1) To offer the analytic analysis for dynamic system frequency in power systems under UV, the stochastic SFR model is proposed for describing the system frequency under UV from generation, loads, measurement and communication. Compared to the previous studies which reported the SFR model [17]–[29], the proposed model has the relevant advantage of being more general and more easily account for the stochastic process formulated by SDEs, which is suitable for the environment with increasing UV. (2) The intra-range probability, which is defined as the probability of the system frequency being in the security range, is presented as the index to assess the impact of UV on system frequency. This probability index can directly assess whether the system frequency is within the security range, which has not been presented in previous related studies [14], [15]. (3) An analytic analysis method is proposed to assess the system frequency under UV, in which the intra-range probability can be calculated analytically. Compared to previous studies focused on the impact of UV on power system [30]–[49], the analysis of the system frequency under UV has not been presented. (4) A meaningful observation that the system frequency under UV has a probabilistic steady-state solution is found, despite that the system frequency dynamically changes over time. As the authors know, such probabilistic steady-state solution about system frequency has not been reported in previous studies yet. (5) When the UV is introduced into the SFR model, impacts of SFR model's parameters on intra-range probability are offered, providing insights for improving the system frequency stability under UV. Compared with the analysis of SFR in [16], the analysis in this paper provides an understanding of the way in which important system parameters affect the frequency response under UV.

The remainder of this paper is organized as follows: Section II presents the system frequency model under UV; Section III proposes the analytic method to analyze the system frequency under UV; Section IV gives simulation cases; Section V offers conclusions.

II. SYSTEM FREQUENCY RESPONSE MODEL UNDER UNCERTAIN VARIABILITY

The SFR model is widely used in system frequency analysis, where the detailed power system model is equivalent to a simplified system [16]. In this section, a stochastic SFR model, which is shown in Fig. 1, is proposed to describe the dynamic system frequency under UV.

The UV is mainly considered as the intermittent power fluctuations of the renewable energy generation and random loads, stochastic errors of measurement, and noise in communication channels.

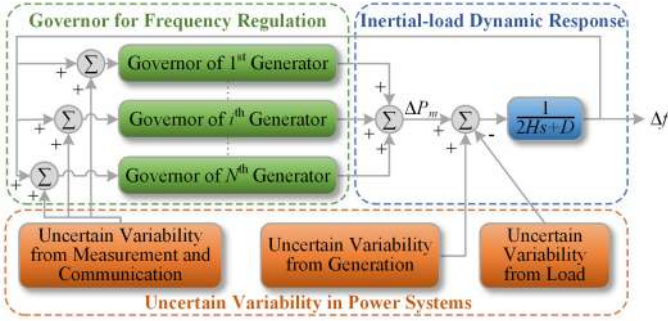


Fig. 1. The SFR model under uncertain variability.

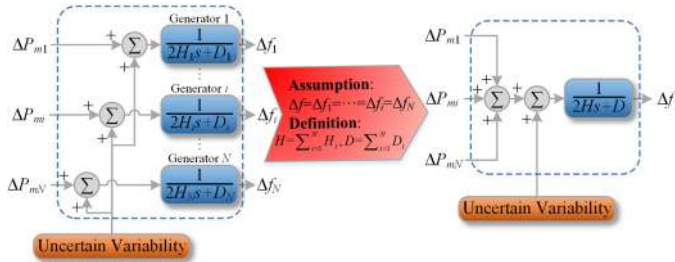


Fig. 2. Model equivalence process of system inertia model under uncertain variability.

A. System Inertia Model Under Uncertain Variability

The SFR model is built based on the system inertia model. The UV in system inertia model mainly comes from the renewable energy generation and active random loads. The classic system inertia model has been presented to analyze the system frequency, when the governor model is ignored. In the classic system inertia model, the system frequency is assumed to be uniform through the whole power system. Furthermore, all synchronous generators and loads are merged to preserve the essence of system frequency response. Due to its generality and simplicity, the classic system inertia model is widely used in under-frequency load shedding, frequency response estimation, and primary frequency regulation, etc. In this paper, all synchronous generators and equivalent loads are merged in the system inertia model, so that the UV from the renewable energy generation and loads can be summed. Fig. 2 shows the process of obtaining the system inertia model under UV from renewable energy generation and random loads.

The system inertia model under UV can be formulated as

$$2Hd\Delta f/dt = \Delta P_m - D\Delta f + \sigma_1 W_1(t) \quad (1)$$

where Δf denotes the system frequency deviation between the system frequency f and its reference value f_0 (i.e., the synchronous system frequency); H denotes the equivalent system inertia, which equals to the sum of system inertia values of all generators in the system; ΔP_m denotes total mechanical power deviation, which is regulated by governors; D denotes the equivalent damping coefficient, which equals to the sum of damping values of all generators in the system; $\sigma_1 W_1(t)$ denotes the UV

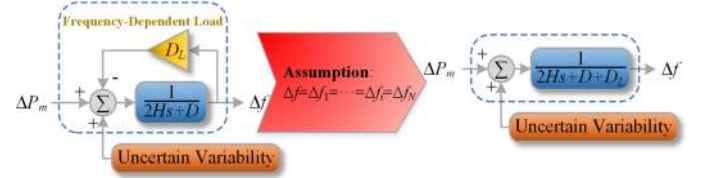


Fig. 3. The frequency-dependent load in the SFR model.

from the generation and loads; σ_1 denotes the UV's intensity; $W_1(t)$ denotes a stochastic process.

B. Governor Model Under Uncertain Variability

The governor model is an important part in the SFR model. The models of governors are added into the system inertia model to include the dynamic response of governor, and then the SFR model is obtained. In the previous studies, many models that describe the detailed dynamic behavior of governors have been proposed. In power systems, major types of governors are included in steam turbines [50]–[52], hydraulic turbines [53], gas turbines [54], nuclear plants [55], etc.

The UV from measurement and communication can be considered in the governor model, which is added to the frequency input signal of governors. The UV is also modeled by stochastic processes, as follows:

$$\Delta f' = \Delta f + \sigma_2 W_2(t) \quad (2)$$

where Δf denotes the real system frequency deviation; $\Delta f'$ denotes the system frequency deviation that a governor receives; $\sigma_2 W_2(t)$ denotes the UV incorporated in the frequency measurement and communication; σ_2 denotes the intensity of the UV; $W_2(t)$ denotes a stochastic process.

C. Frequency-Dependent Loads in the SFR Model

In practice, some power systems may contain frequency-dependent loads [56], which are sensitive to system frequency deviation. Let D_L denote the load-frequency coefficient, and then the power variations of the frequency-dependent loads around the operating point can be expressed as

$$\Delta P_L = D_L \Delta f \quad (3)$$

The frequency-dependent loads can be considered in the SFR model by revising the damping coefficient D to the equivalent damping coefficient $D + D_L$. The process of adding a frequency-dependent load in the SFR model is shown in Fig. 3.

D. Stochastic Differential Equations

To develop the theoretical stochastic model, the UV is described as stochastic processes, and then the SFR model under UV can be formulated by SDEs. In the SFR model, there is only linear relation [16]. Thus, when the UV is introduced into the SFR model, the stochastic model can be expressed as a set of linearized SDEs:

$$d\mathbf{X}(t) = \mathbf{A}\mathbf{X}(t)dt + \mathbf{K}d\mathbf{B}(t) \quad (4)$$

where $\mathbf{X}(t)$ is the vector of system states in the SFR model, in which one of the entries is the system frequency deviation Δf ; \mathbf{A} is the state matrix of the linearized system; $\mathbf{KdB}(t)$ is the vector of UV; \mathbf{K} is the covariance matrix of UV, which describes the intensity and correlation of UV; $\mathbf{B}(t)$ is a vector whose entries are independent standard Wiener processes.

III. ANALYTIC ANALYSIS OF SYSTEM FREQUENCY UNDER UNCERTAIN VARIABILITY

In this section, the systemic analytic analysis of dynamic system frequency under UV is performed.

A. Probability Density Function of the System Frequency Deviation Over Time

By using the linearized stochastic theory [44], the solution of (4) can be deduced as

$$\mathbf{X}(t) = e^{\mathbf{A}(t-t_0)} \mathbf{X}(t_0) + \int_{t_0}^t e^{\mathbf{A}(t-s)} \mathbf{KdB}(s) \quad (5)$$

where $e^{\mathbf{A}(t-t_0)}$ is an exponential function of the n th-order square matrix $\mathbf{A}(t-t_0)$, and $e^{\mathbf{A}(t-t_0)} = \sum_{n=0}^{+\infty} \{\mathbf{A}(t-t_0)\}^n / n!$.

It is proved that $\int_{t_0}^t e^{\mathbf{A}(t-s)} \mathbf{KdB}(s)$ follows the Gaussian distribution [57], so the system states in $\mathbf{X}(t)$ also follow Gaussian distributions. The mean and variance are two key parameters for Gaussian distributions. The mean and covariance of system states (5) over time can be analytically solved as follows (the derivation is presented in Appendix):

$$\begin{cases} \text{Mean}[\mathbf{X}(t)] = e^{\mathbf{A}(t-t_0)} \mathbf{X}(t_0) \\ \text{Var}[\mathbf{X}(t)] = \mathbf{P} \{ [\mathbf{P}^{-1} \mathbf{K} \mathbf{K}^T (\mathbf{P}^{-1})^T] \circ \mathbf{J} \} \mathbf{P}^T \end{cases} \quad (6)$$

where $\text{Mean}[\mathbf{X}(t)]$ is the mean vector of $\mathbf{X}(t)$; $\text{Var}[\mathbf{X}(t)]$ is the variance-covariance matrix of $\mathbf{X}(t)$; \circ is the Hadamard product [58]; \mathbf{J} is a matrix whose (i, j) th entry is $[e^{(\lambda_i + \lambda_j)(t-t_0)} - 1] / (\lambda_i + \lambda_j)$; λ_i (λ_j) is the i th (j th) eigenvalue of \mathbf{A} ; \mathbf{P} is a square matrix, whose columns are the independent eigenvectors of \mathbf{A} ; in other words, λ_i (λ_j) equals to the i th (j th) diagonal entries of $\mathbf{\Lambda}$, and $\mathbf{P} \mathbf{\Lambda} \mathbf{P}^{-1} = \mathbf{A}$.

Given that the system states in $\mathbf{X}(t)$ obey Gaussian distributions at a certain time, one can deduce the probability density function (PDF) of the system frequency deviation over time as

$$f_{PDF}(\Delta f) = e^{-(\Delta f - \mu)^2 / (2\sigma^2)} / \sqrt{2\pi\sigma^2} \quad (7)$$

where $f_{PDF}(\Delta f)$ denotes the PDF of system frequency deviation Δf ; σ^2 is the variance of system frequency deviation, which is a diagonal entry of $\text{Var}[\mathbf{X}(t)]$ in (6); μ is the mean of system frequency deviation, which is a diagonal entry of $\text{Mean}[\mathbf{X}(t)]$ in (6).

B. Intra-Range Probability of System Frequency Deviation

In the power system suffering a deterministic disturbance (e.g., a gradual load decrease or a sudden load loss), the effect of this disturbance is smaller when the disturbance is weaker. When the same power system is subjected to UV, the very small

UV could bring considerable effects [59]. In stochastic theory, it is reasonable that the effect of UV should be described by the statistical value. In practice, it is desired that the system frequency needs to be maintained within the certain security range to meet the frequency performance criteria [14]. However, it becomes a random problem to determine whether the system frequency is in the certain range, when a power system is subjected to the UV. The probability that the system frequency deviation is within a certain security range is defined as the intra-range probability in this paper, which is defined as follows

$$P(t) = \text{Prob}\{f_{\min} < \Delta f(t) < f_{\max}\} \quad (8)$$

where $\Delta f(t)$ is the system frequency deviation at time t ; f_{\min} and f_{\max} are the boundaries of the frequency deviation range; and $\text{Prob}\{f_{\min} < \Delta f(t) < f_{\max}\}$ is the probability of system frequency deviation $\Delta f(t)$ being in the security range $[f_{\min}, f_{\max}]$ at time t .

In a power system, it makes sense that the effects of UV are weaker when the intra-range probability is larger. The intra-range probability can be regarded as a good index to assess the impact of UV on system frequency.

Furthermore, the intra-range probability of the system frequency deviation can be expressed as the integral of the PDF $f_{PDF}(\Delta f)$ (7), as follows:

$$\begin{aligned} P(t) &= \text{Prob}\{f_{\min} < \Delta f(t) < f_{\max}\} \\ &= \int_{f_{\min}}^{f_{\max}} f_{PDF}(\Delta f) d\Delta f \\ &= \int_{f_{\min}}^{f_{\max}} e^{-(\Delta f - \mu)^2 / (2\sigma^2)} / \sqrt{2\pi\sigma^2} d\Delta f. \end{aligned} \quad (9)$$

C. Steady-State Intra-Range Probability

In this study, the system is assumed to be stable initially, so all eigenvalues of the corresponding system state matrix \mathbf{A} in (4) have negative real parts. Furthermore, one obtains

$$\begin{cases} \lim_{t \rightarrow +\infty} e^{\lambda_i t} = 0 \\ \lim_{t \rightarrow +\infty} e^{\mathbf{A}t} = \mathbf{O} \end{cases} \quad (10)$$

where \mathbf{O} denotes a zero matrix.

Based on (10), the limit of the mean vector in (6) can be deduced as follows:

$$\lim_{t \rightarrow +\infty} \text{Mean}[\mathbf{X}(t)] = \lim_{t \rightarrow +\infty} e^{\mathbf{A}(t-t_0)} \mathbf{X}(t_0) = \mathbf{O}. \quad (11)$$

Because the limit value of $e^{\lambda_i t}$ exists (shown in (10)), the limit of the variance-covariance matrix in (6) can be obtained. In (6), the covariance matrix of UV \mathbf{K} is assumed to be constant; \mathbf{P} is the eigenvector of the state matrix \mathbf{A} which is constant in a specific simulation system; \mathbf{J} is the only part changing with the time, due to the existence of time t . Based on (10), the limit of

\mathbf{J} can be obtained as the following formulation

$$\begin{aligned} \lim_{t \rightarrow +\infty} \mathbf{J}(i, j) &= \lim_{t \rightarrow \infty} \left[e^{(\lambda_i + \lambda_j)(t-t_0)} - 1 \right] / (\lambda_i + \lambda_j) \\ &= \left[\lim_{t \rightarrow \infty} e^{(\lambda_i + \lambda_j)(t-t_0)} - 1 \right] / (\lambda_i + \lambda_j) \\ &= -1 / (\lambda_i + \lambda_j) \\ &= \mathbf{T}(i, j) \end{aligned} \quad (12)$$

where $\mathbf{J}(i, j)$ is the (i, j) th entry of \mathbf{J} ; and \mathbf{T} is defined as a matrix whose the (i, j) th entry $\mathbf{T}(i, j)$ is $-1 / (\lambda_i + \lambda_j)$.

Substituting (12) into $\text{Var}[\mathbf{X}(t)]$ in (6), one can deduce the limit of $\text{Var}[\mathbf{X}(t)]$ as follows:

$$\begin{aligned} \lim_{t \rightarrow +\infty} \text{Var}[\mathbf{X}(t)] &= \mathbf{P} \left\{ \left[\mathbf{P}^{-1} \mathbf{K} \mathbf{K}^T (\mathbf{P}^{-1})^T \right] \circ \lim_{t \rightarrow \infty} \mathbf{J} \right\} \mathbf{P}^T \\ &= \mathbf{P} \left\{ \left[\mathbf{P}^{-1} \mathbf{K} \mathbf{K}^T (\mathbf{P}^{-1})^T \right] \circ \mathbf{T} \right\} \mathbf{P}^T. \end{aligned} \quad (13)$$

In (13), one of the diagonal entry in $\lim_{t \rightarrow +\infty} \text{Var}[\mathbf{X}(t)]$ is the steady-state variance of the system frequency deviation; and the steady-state mean of the system frequency deviation equals to zero according to (11). Furthermore, based on (9), the steady-state intra-range probability of the system frequency deviation can be obtained as follows:

$$P(t) = \int_{f_{\min}}^{f_{\max}} e^{-\Delta f^2 / (2\sigma_{\text{lim}}^2)} / \sqrt{2\pi\sigma_{\text{lim}}^2} d\Delta f. \quad (14)$$

where σ_{lim} is the steady-state variance of the system frequency deviation.

IV. VALIDATIONS

To verify the proposed analytic method, two simulation cases are adopted in this paper. All simulations are conducted on a computer with a 2.69 GHz CPU and 8 GB memory.

A. Procedure of the Proposed Analytic Analysis Method and Monte Carlo Simulation

The procedure of the proposed analytic analysis is outlined below and shown in Fig. 4.

- Step 1:* Build the stochastic model of the power system under UV by statistical data.
- Step 2:* Obtain the corresponding SFR model under UV for analyzing the system frequency deviation.
- Step 3:* Solve the mean and variance of the system frequency deviation over time based on the proposed method.
- Step 4:* Deduce the PDF of the system frequency deviation over time by using the Gaussian distribution.
- Step 5:* Calculate the intra-range probability of the system frequency deviation by the integral of the system frequency deviation's PDF.

In this study, Monte Carlo simulation is utilized to compare with the proposed method. Monte Carlo simulation means the repeated simulation of the power system model under UV and the statistical analysis. The procedure of Monte Carlo simulation is outlined below and shown in Fig. 5.

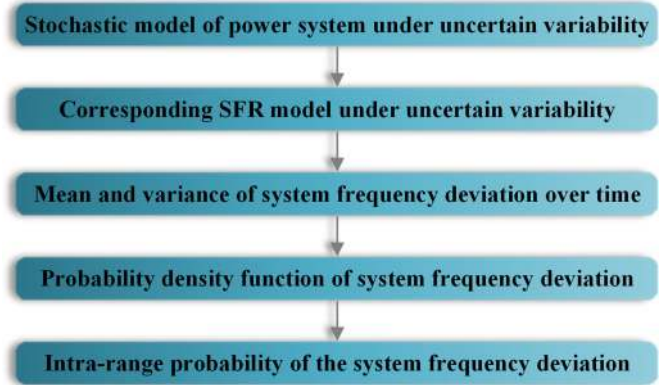


Fig. 4. The procedure of the proposed analytic analysis method for the intra-range probability of the system frequency deviation under uncertain variability.

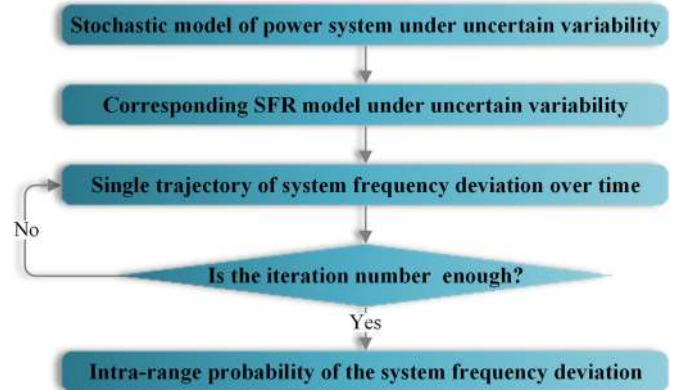


Fig. 5. The procedure of the Monte Carlo simulation for the intra-range probability of system frequency deviation under uncertain variability.

- Step 1:* Build the stochastic model of the power system under UV by statistical data.
- Step 2:* Obtain the corresponding SFR model under UV for analyzing the system frequency deviation.
- Step 3:* Simulate the SFR model for one time and obtain a single trajectory of the system frequency deviation.
- Step 4:* Execute Step 3, if the iteration number is not enough; go to Step 5, if the iteration number is enough.
- Step 5:* Calculate the intra-range probability of the system frequency trajectory by judging whether the system frequency trajectory is in the security range.

From the procedures shown in Figs. 4–5, it can be clearly seen that the biggest difference between the Monte Carlo simulation and the proposed method is whether there is the iteration simulation. The iteration simulation is the most time-consuming part of Monte Carlo simulation. In Monte Carlo simulation, each one trial provides the behavior of a single system frequency deviation trajectory, so multiple trials are needed to obtain statistical information of the system frequency in the system under UV. Due to the multiple trials, the burdensome computation makes Monte Carlo simulation has low efficiency. Moreover, because of the unclear impact mechanism, Monte Carlo simulation is like a “black box.” It is known that Monte Carlo simulation has

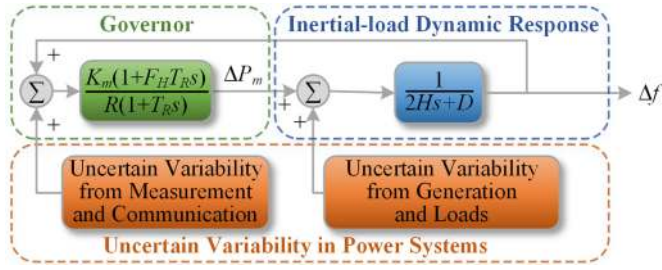


Fig. 6. A typical SFR model under uncertain variability.

 TABLE I
 PARAMETERS OF A TYPICAL SFR MODEL

R	H	K_m	F_H	T_R	D
0.05	4	0.95	0.3	8	1

advantages on good adaptabilities to system models, but the low computational efficiency and unclear impact mechanism often make it undesirable. It is desired to develop an analytic method, which can provide the statistical information of the stochastic system directly. The analytic analysis method proposed in this paper provides such a method, which can offer the final results directly without iterations.

B. A Typical SFR Model Under Uncertain Variability

A typical SFR model in [16] is simulated as the first case, whose framework is shown in Fig. 6.

The parameters of this typical SFR model is shown in Table I, which are from the reference [16] directly. The original case does not include UV. In this paper, the UV is added, which is from the renewable energy generation, random loads, stochastic errors in measurement, and noise in communication channels.

This SFR model under UV shown in Fig. 6 can be formulated as

$$\begin{cases} T_R \dot{t}_g = (1 - F_H)[\Delta f + \sigma_2 W_2(t)]/R - t_g \\ 2H \Delta \dot{f} = -D \Delta f - K_m F_H [\Delta f + \sigma_2 W_2(t)]/R - K_m t_g \\ \quad + \sigma_1 W_1(t) \end{cases} \quad (15)$$

where R denotes the droop; t_g denotes the system state of the governor; T_R denotes the reheat time constant; F_H denotes the fraction of total power generated by the high-pressure turbine; and K_m denotes the mechanical power gain factor; $\sigma_1 W_1(t)$ denotes the UV from the generation and loads, in which σ_1 is the intensity of the UV and $W_1(t)$ is a stochastic process; $\sigma_2 W_2(t)$ denotes the UV incorporated in the frequency measurement and communication, in which σ_2 is the intensity of the UV and $W_2(t)$ is a stochastic process. In this case, the intensity of the UV from the generation and load is set as 0.01; the intensity of the UV from the measurement and communication is set to 0.0001.

Furthermore, the SFR model under UV (15) can be formulated in a matrix form, which is a set of linearized SDEs (4). The system state matrix \mathbf{A} and the covariance matrix of SCDs

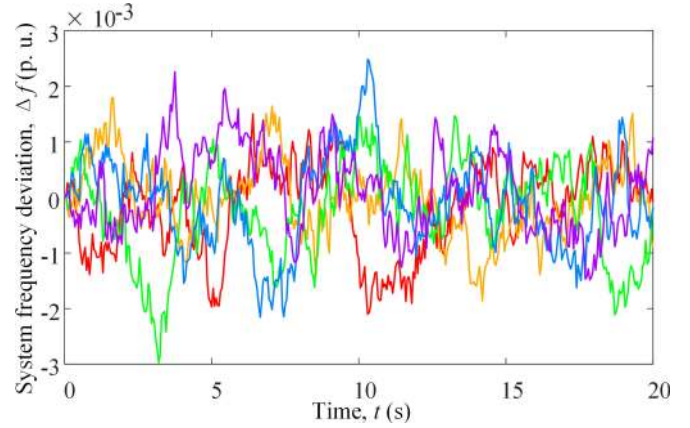


Fig. 7. Five trajectories of system frequency deviation under the uncertain variability.

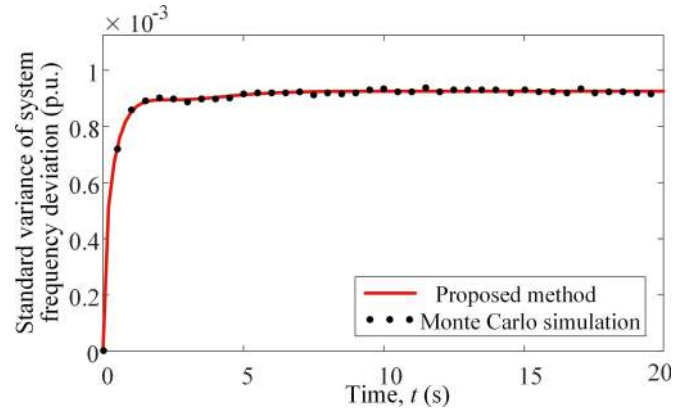


Fig. 8. The standard variance of the system frequency deviation over time in a typical SFR model under UV.

\mathbf{K} can be expressed as follows:

$$\begin{cases} \mathbf{A} = \begin{bmatrix} -1/T_R & (1 - F_H)/(RT_R) \\ -K_m/(2H) & -(D + K_m F_H/R)/(2H) \end{bmatrix} \\ \mathbf{K} = \begin{bmatrix} 0 & \sigma_2(1 - F_H)/(RT_R) \\ \sigma_1/(2H) & -\sigma_2 K_m F_H/(2HR) \end{bmatrix} \end{cases} \quad (16)$$

Using Monte Carlo simulation, five different trajectories of system frequency deviation under the UV are shown in Fig. 7 with different colors. Due to the introduction of UV, the trajectories of the system frequency deviation are randomly fluctuant, from which it is hard to obtain insights directly.

Based on Monte Carlo simulation and the proposed method, the standard variance of system frequency deviation over time is calculated and shown in Fig. 8. The simulation number of the Monte Carlo simulation here is set to 10000. It can be seen that the results of the proposed method agree well with those of Monte Carlo simulation.

Based on the calculated standard variance of system frequency deviation, the PDF of the system frequency deviation over time can be obtained by (7), which is shown in Fig. 9. Clearly, the PDF of the system frequency deviation converges

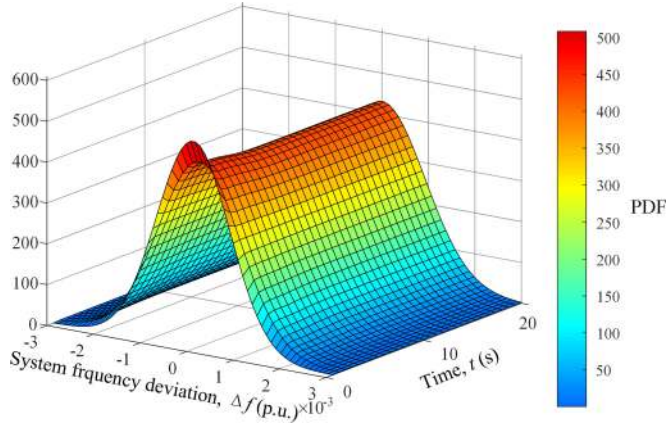


Fig. 9. Probability density function of system frequency deviation over time.

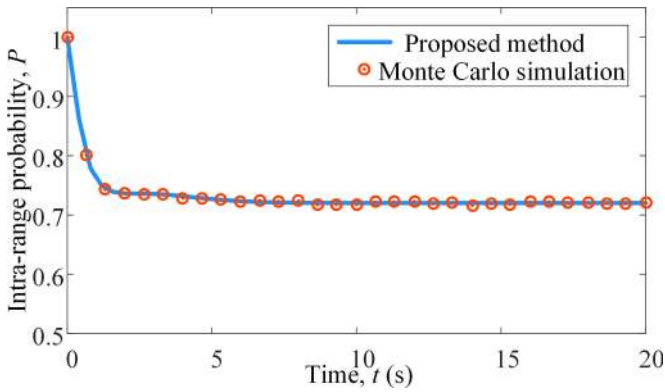


Fig. 10. Intra-range probability simulated by Monte Carlo simulation and the proposed method.

to a certain distribution over time, which means the system frequency deviation has a stationary distribution.

In this paper, the security range of the system frequency deviation is set to $[-0.001, 0.001]$ for this simulation case. Based on (9), the intra-range probability of the system frequency deviation can be calculated analytically, which is shown in Fig. 10. Meanwhile, the Monte Carlo simulation is carried out, whose results are also shown in Fig. 10. Clearly, it can be seen that the results from the proposed method are much close to those from Monte Carlo simulation, which illustrates the accuracy of the proposed method. Furthermore, it can be found that the intra-range probability has a limit, which is called the probabilistic steady-state solution. This probabilistic steady-state solution means that the system frequency deviation under UV always fluctuates, but its statistics are steady. This observation can be theoretically explained by (10)–(14) in the proposed method. By (14), it is easy to obtain the limit of intra-range probability directly.

C. The Impact of SFR Model's Parameters on Intra-Range Probability

In this section, the parameters of the SFR model (i.e., R, H, K_m, F_H , and D) are tuned, and then corresponding

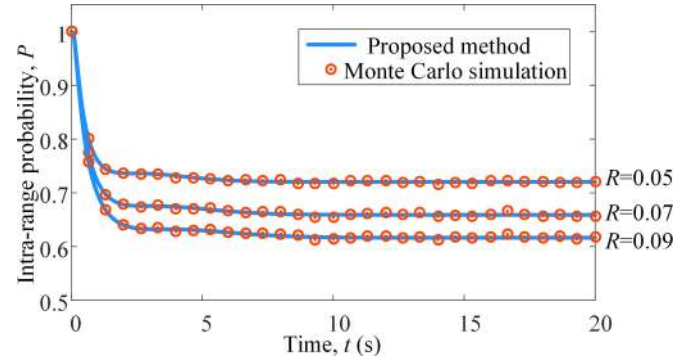


Fig. 11. The intra-range probability of system frequency under different R .

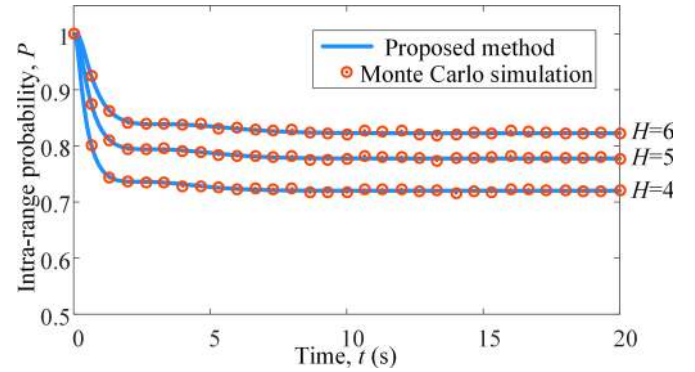


Fig. 12. The intra-range probability of system frequency under different H .

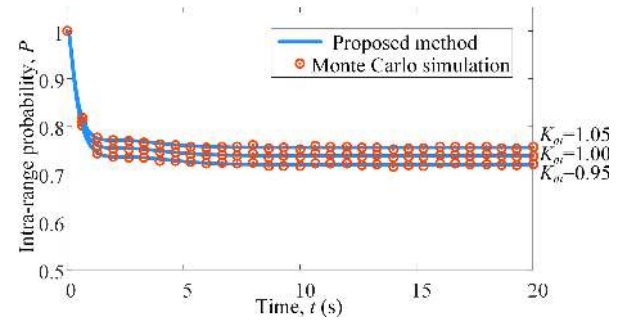


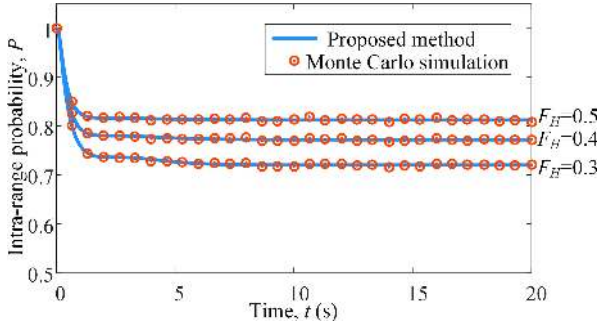
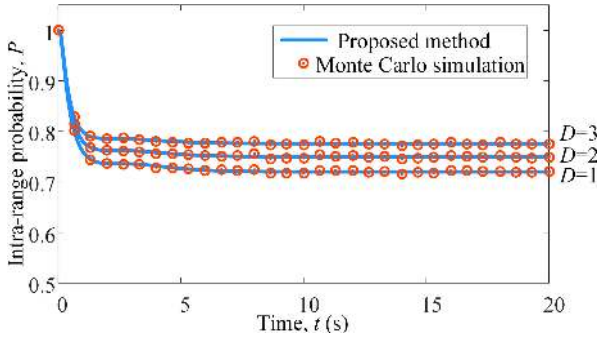
Fig. 13. The intra-range probability of system frequency under different K_m .

intra-range probability curves are calculated to illustrate the impacts of these parameters on the intra-range probability.

The value of R varies from 0.05 to 0.09 with increments of 0.02 per unit. The intra-range probability curves are shown in Fig. 11. It can be detected that the system has the higher intra-range probability, when the value of R is smaller.

The value of H varies from 4 to 6 in increments of 1 per unit. The intra-range probability curves are shown in Fig. 12. It can be detected that the system has the higher intra-range probability, when the value of H is larger.

The value of K_m varies from 0.95 to 1.05 in increments of 0.05 per unit. The intra-range probability curves are shown in Fig. 13. It can be detected that the system has the higher intra-range probability, when the value of K_m is larger.


 Fig. 14. The intra-range probability of system frequency under different F_H .

 Fig. 15. The intra-range probability of system frequency under different D .

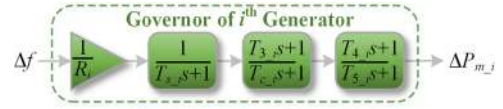
The value of F_H varies from 0.3 to 0.5 in increments of 0.1 per unit. The intra-range probability curves are shown in Fig. 14. It can be detected that the system has the higher intra-range probability, when the value of F_H is larger.

The value of D varies from 1 to 3 in increments of 1 per unit. The intra-range probability curves are shown in Fig. 15. It can be detected that the system has the higher intra-range probability, when the value of D is larger.

From Figs. 11–15, the insights for improving the system frequency characteristics can be found by decreasing R , increasing H , increasing K_m , increasing F_H , and increasing D . Meanwhile, it can be seen that the proposed method still has high accuracy under different R, H, K_m, F_H , and D . Furthermore, the observation that the intra-range probability has the probabilistic steady-state solution can be seen even under different R, H, K_m, F_H , and D .

D. Scalability of the Proposed Analytic Method in a Large Power System

In this paper, the simulation case of Iceland electricity transmission network is employed to verify the scalability of the proposed analytic method in a larger power system. As a simulation system in Power System Analysis Toolbox (PSAT), the Iceland electricity transmission network consists of 118 nodes, 206 branches, and 35 generators. Its parameters can be found in [60]. Since the original data does not include the damping information, damping coefficients are assumed to be 0.5 M (i.e., the damping coefficient of every generator is equal to a half of the corresponding inertia coefficient). Moreover, the UV from the renewable energy generation, random loads, stochastic


 Fig. 16. Governor model of i th Generator.

errors in measurement, and noise in communication channels is introduced to this system. The intensity of the UV from the generation and load is set to 0.01 P_m . In this simulation case of Iceland electricity transmission network in PSAT, the per unit value of the total mechanical power is 18.78, so the intensity of the UV from the generation and load is set to 0.2 (close to 0.1878). The intensity of the UV from the measurement and communication is set to 0.0001 f_0 . In this simulation case of Iceland electricity transmission network, the per unit value of the synchronous system frequency f_0 is 1, so the intensity of the UV from the measurement and communication is set to 0.0001. It should be noted that the proposed method still can have high accuracy, no matter how the intensity of the UV is set. In this paper, the intensity values of UV are just chosen as some reasonable values. Researchers who want to use the proposed method can portray the intensity of UV according to their needs.

In this system, all governors are thermal generators. In PSAT, the governor models of thermal generators are called as the type I turbine governor [61]. The diagram for the model of the type I turbine governor is shown in Fig. 16.

According to Fig. 16, the governor model of i th generator can be expressed as follows:

$$\begin{cases} T_{in} = -\Delta f/R \\ \dot{t}_{g1} = (T_{in} - t_{g1})/T_s \\ \dot{t}_{g2} = [(1 - T_3/T_c)t_{g1} - t_{g2}]/T_c \\ \dot{t}_{g3} = [(1 - T_4/T_5)(t_{g2} + t_{g1}T_3/T_c) - t_{g3}]/T_5 \\ \Delta P_m = t_{g3} + (t_{g2} + t_{g1}T_3/T_c)T_4/T_5 \end{cases} \quad (17)$$

where R denotes the droop; t_{g1}, t_{g2} , and t_{g3} denote system states of the governor; T_s denotes the governor time constant; T_c denotes the servo time constant; T_3 denotes the transient gain time constant; T_4 denotes the power fraction time constant; and T_5 denotes the reheat time constant.

Furthermore, the SFR model of Iceland electricity transmission network is used to analyze the system frequency deviation under UV. In other words, the Iceland electricity transmission network is equivalent to the model shown in Fig. 1, and models of the governors are illustrated in Fig. 16 and expressed by (17). Then, the SFR model of this system under UV can be formulated in the form of linearized SDEs (4).

Using the proposed analytic method in this paper and Monte Carlo simulation, the standard variance of the system frequency deviation under the UV is calculated and shown in Fig. 17. The results from the proposed method still agree well with those from Monte Carlo simulation. Furthermore, the intra-range probability under UV can be calculated from (9), when the standard deviation of the system frequency deviation over time is obtained. In Fig. 18, the intra-range probability curves from the proposed method and Monte Carlo simulation are illustrated.

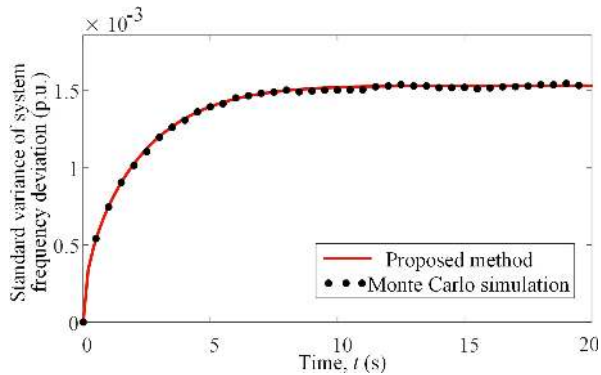


Fig. 17. The standard variance of the system frequency deviation over time in Iceland electricity transmission network under uncertain variability.

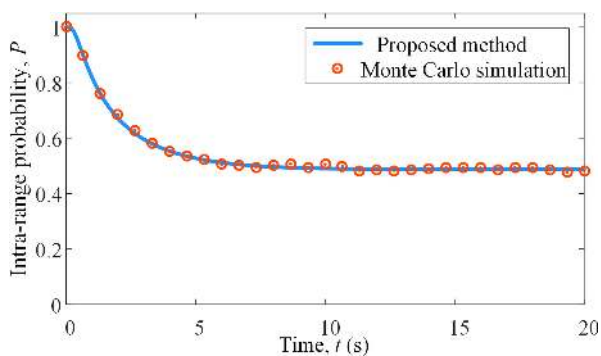


Fig. 18. Intra-range probability of the system frequency in Iceland electricity transmission network under uncertain variability.

TABLE II
COMPUTATION COMPARISONS BETWEEN THE MONTE CARLO
SIMULATION AND THE PROPOSED METHOD

	Monte Carlo simulation				Proposed method
	Simulation number	100	1000	10000	
Computational time(s)	17	179	1606	16520	0.1
Result at $t=20s$	0.51	0.479	0.488	0.487	0.487

It can be seen that the proposed method achieves the satisfied accuracy. Meanwhile, the same observation is illustrated again, which shows that the intra-range probability of system frequency deviation has the probabilistic steady-state solution.

Besides the accuracy, the computational efficiency is critical for an analysis method in practice. To obtain the intra-range probability at $t = 20$ s of the Iceland electricity transmission network simulation case under UV, the computational time of the proposed method is 0.1 s, but it takes 1606s in Monte Carlo simulation with iteration 10000 and time step 0.001 s. Meanwhile, the result accuracy of Monte Carlo simulation with this configuration is still not extremely high, see Table II. Hence, the proposed method significantly saves the calculation time, when a larger power system under UV needs to be analyzed. Considering the increasing UV in future power grids, this improvement in computation efficiency is extremely beneficial to system situational awareness and reliability assessment in control rooms.

V. CONCLUSIONS

With the ever-growing uncertainty in power systems, system frequency issues under UV are of concern. This paper sets out to deal with system frequency issues under UV, which achieves five main contributions as follows:

- 1) Described by the SDEs, the stochastic SFR model is proposed for analyzing the system frequency under UV from generation, loads, measurement and communication. Compared to the classic SFR model, the proposed stochastic SFR model has advantages on considering the UV, which is critical for the power system in an environment with the increasing UV.
- 2) The intra-range probability, which is defined as the probability of system frequency deviation being in the security range, is presented as the index to assess the impact of UV on the system frequency. The intra-range probability is beneficial for analyzing the instantaneous and short-term system frequency stability under UV, which can directly assess whether the system frequency deviation is within the security range.
- 3) An analytic method is proposed to assess the system frequency under UV, in which the intra-range probability can be calculated analytically. Compared with the Monte Carlo simulation, the proposed analytic method shows two significant advantages including the clear mechanism and high efficiency with the almost the same accuracy. The high efficiency is very beneficial for users, when many plans need to be compared or when the analysis must be quick in the system frequency assessment under UV.
- 4) It is found that the system frequency deviation under UV has a probabilistic steady-state solution, despite that the system frequency dynamically changes over time. This meaningful observation can theoretically explain the characteristics of some system frequency fluctuations in actual power systems. Even though the system frequency always fluctuates in power systems, such observation about the probabilistic steady-state solution of system frequency has not been reported yet.
- 5) When the UV is introduced into the SFR model, the impacts of SFR model's parameters on intra-range probability are offered, providing insights for improving the system frequency stability under UV. These insights also offer an understanding of the way in which important system parameters affect the system frequency response under UV.

With the rapid development of power systems, UV is challenging power systems theoretically and practically. System frequency issues under UV are of concern for the power system operators. An accurate and efficient analytic method for analyzing system frequency under UV is much desired. The method proposed in this paper can help well in this regard.

APPENDIX

In this appendix, the mean and covariance of system states along with the time are deduced.

Based on the solution of linearized SDEs (5), the mean of system state over time can be defined as follows:

$$\begin{aligned} \text{Mean}[\mathbf{X}(t)] &= E \left[e^{\mathbf{A}(t-t_0)} \mathbf{X}(t_0) + \int_{t_0}^t e^{\mathbf{A}(t-s)} \mathbf{K} d\mathbf{B}(s) \right] \\ &= E \left[e^{\mathbf{A}(t-t_0)} \mathbf{X}(t_0) \right] + E \left[\int_{t_0}^t e^{\mathbf{A}(t-s)} \mathbf{K} d\mathbf{B}(s) \right] \end{aligned} \quad (\text{A-1})$$

where E denotes the mean.

According to the theory of stochastic calculus [57], the mean of system state over time can be deduced as the following form

$$\begin{aligned} \text{Mean}[\mathbf{X}(t)] &= E \left[e^{\mathbf{A}(t-t_0)} \mathbf{X}(t_0) \right] \\ &\quad + E \left\{ \sum_{i=0}^{k-1} e^{\mathbf{A}(t-t_i)} \mathbf{K} [\mathbf{B}(t_{i+1}) - \mathbf{B}(t_i)] \right\} \\ &= \sum_{i=0}^{k-1} \left\{ e^{\mathbf{A}(t-t_i)} \mathbf{K} E [\mathbf{B}(t_{i+1}) - \mathbf{B}(t_i)] \right\} \\ &= E \left[e^{\mathbf{A}(t-t_0)} \mathbf{X}(t_0) \right]. \end{aligned} \quad (\text{A-2})$$

Based on (5), the covariance of system states over time can be defined as

$$\begin{aligned} \text{Var}[\mathbf{X}(t)] &= E \left\{ \left\{ \mathbf{X}(t) - E[\mathbf{X}(t)] \right\} \left\{ \mathbf{X}(t) - E[\mathbf{X}(t)] \right\}^T \right\} \\ &= E \left\{ \left[\int_{t_0}^t e^{\mathbf{A}(t-s)} \mathbf{K} d\mathbf{B}(s) \right] \left[\int_{t_0}^t e^{\mathbf{A}(t-s)} \mathbf{K} d\mathbf{B}(s) \right]^T \right\}. \end{aligned} \quad (\text{A-3})$$

According to the theory of stochastic calculus [57], the following equation can be deduced from (A-3)

$$\begin{aligned} \text{Var}[\mathbf{X}(t)] &= E \left\{ \left\{ \sum_{i=0}^{k-1} e^{\mathbf{A}(t-t_i)} \mathbf{K} [\mathbf{B}(t_{i+1}) - \mathbf{B}(t_i)] \right\} \right. \\ &\quad \left. \times \left\{ \sum_{j=0}^{k-1} e^{\mathbf{A}(t-t_j)} \mathbf{K} [\mathbf{B}(t_{j+1}) - \mathbf{B}(t_j)] \right\}^T \right\} \\ &= \sum_{0 \leq i, j \leq k-1} \left\langle e^{\mathbf{A}(t-t_i)} \mathbf{K} E \left\{ [\mathbf{B}(t_{i+1}) - \mathbf{B}(t_i)] \right. \right. \\ &\quad \left. \left. \times [\mathbf{B}(t_{j+1}) - \mathbf{B}(t_j)]^T \right\} \mathbf{K}^T e^{\mathbf{A}^T(t-t_j)} \right\rangle \\ &= \sum_{0 \leq i, j \leq k-1, \text{ and } i=j} \left\langle e^{\mathbf{A}(t-t_i)} \mathbf{K} E \left\{ [\mathbf{B}(t_{i+1}) - \mathbf{B}(t_i)] \right. \right. \\ &\quad \left. \left. \times [\mathbf{B}(t_{j+1}) - \mathbf{B}(t_j)]^T \right\} \mathbf{K}^T e^{\mathbf{A}^T(t-t_j)} \right\rangle \\ &\quad + \sum_{0 \leq i, j \leq k-1, \text{ and } i \neq j} \left\langle e^{\mathbf{A}(t-t_i)} \mathbf{K} E \left\{ [\mathbf{B}(t_{i+1}) - \mathbf{B}(t_i)] \right. \right. \\ &\quad \left. \left. \times [\mathbf{B}(t_{j+1}) - \mathbf{B}(t_j)]^T \right\} \mathbf{K}^T e^{\mathbf{A}^T(t-t_j)} \right\rangle \end{aligned} \quad (\text{A-4})$$

where $t_k = t$.

By the definition of Wiener processes [57], one obtains

$$\begin{aligned} E\{[\mathbf{B}(t_{i+1}) - \mathbf{B}(t_i)][\mathbf{B}(t_{j+1}) - \mathbf{B}(t_j)]^T\} \\ = \begin{cases} t_{i+1} - t_i, & \text{if } i = j \\ 0, & \text{if } i \neq j \end{cases}. \end{aligned} \quad (\text{A-5})$$

Substituting (A-5) in (A-4), the following equation can be deduced

$$\begin{aligned} \text{Var}[\mathbf{X}(t)] &= \sum_{i=0}^{k-1} \left\{ e^{\mathbf{A}(t-t_i)} \mathbf{K} \mathbf{K}^T e^{\mathbf{A}^T(t-t_i)} (t_{i+1} - t_i) \right\} \\ &= \int_{t_0}^t e^{\mathbf{A}(t-s)} \mathbf{K} \mathbf{K}^T e^{\mathbf{A}^T(t-s)} ds. \end{aligned} \quad (\text{A-6})$$

In (A-6), there is the integral leading the calculation difficulty. In the following, an analytic expression of the system state covariance including only elementary arithmetic operations (i.e., no integral operations) is deduced, based on the matrix operations.

Based on the eigendecomposition, the system state matrix \mathbf{A} is formulated as follows:

$$\mathbf{A} = \mathbf{P} \mathbf{\Lambda} \mathbf{P}^{-1} \quad (\text{A-7})$$

where $\mathbf{\Lambda}$ is the eigenvalue matrix, which is a diagonal matrix $\text{diag}[\lambda_1, \lambda_2, \dots, \lambda_i, \dots]$; and \mathbf{P} is the similarity transformation from \mathbf{A} to $\mathbf{\Lambda}$, where the columns are the eigenvectors.

Substituting (A-7) into $e^{\mathbf{A}(t-s)}$, one obtains

$$e^{\mathbf{A}(t-s)} = \mathbf{P} \mathbf{\Gamma} \mathbf{P}^{-1} \quad (\text{A-8})$$

where $\mathbf{\Gamma} = \text{diag}[e^{\lambda_1 t - \lambda_1 s}, e^{\lambda_2 t - \lambda_2 s}, \dots, e^{\lambda_i t - \lambda_i s}, \dots]$.

Incorporating (A-8) into (A-6) $\text{Var}[\mathbf{X}(t)]$, the following equation can be deduced

$$\begin{aligned} \text{Var}[\mathbf{X}(t)] &= \int_{t_0}^t \mathbf{P} \mathbf{\Gamma} \mathbf{P}^{-1} \mathbf{K} \mathbf{K}^T (\mathbf{P}^{-1})^T \mathbf{\Gamma}^T \mathbf{P}^T ds \\ &= \mathbf{P} \left[\int_{t_0}^t \mathbf{\Gamma} \mathbf{P}^{-1} \mathbf{K} \mathbf{K}^T (\mathbf{P}^{-1})^T \mathbf{\Gamma}^T ds \right] \mathbf{P}^T. \end{aligned} \quad (\text{A-9})$$

Let \mathbf{F} and \mathbf{G} denote the matrix $\mathbf{P}^{-1} \mathbf{K} \mathbf{K}^T (\mathbf{P}^{-1})^T$ and $\mathbf{\Gamma} \mathbf{P}^{-1} \mathbf{K} \mathbf{K}^T (\mathbf{P}^{-1})^T \mathbf{\Gamma}^T$, respectively. Considering that $\mathbf{\Gamma}$ is a diagonal matrix, one deduces

$$\mathbf{G}(i, j) = \mathbf{F}(i, j) e^{\lambda_i t - \lambda_i s} e^{\lambda_j t - \lambda_j s} = \mathbf{F}(i, j) e^{(\lambda_i + \lambda_j)(t-s)} \quad (\text{A-10})$$

where $\mathbf{F}(i, j)$ and $\mathbf{G}(i, j)$ are the (i, j) th entry of \mathbf{F} and \mathbf{G} (in the i th row and j th column), respectively.

Let \mathbf{H} be the matrix $\int_{t_0}^t \mathbf{\Gamma} \mathbf{P}^{-1} \mathbf{K} \mathbf{K}^T (\mathbf{P}^{-1})^T \mathbf{\Gamma}^T ds$, and the following equation can be deduced

$$\begin{aligned} \mathbf{H}(i, j) &= \int_{t_0}^t \mathbf{G}(i, j) ds = \int_{t_0}^t \mathbf{F}(i, j) e^{(\lambda_i + \lambda_j)(t-s)} ds \\ &= \mathbf{F}(i, j) \left[e^{(\lambda_i + \lambda_j)(t-t_0)} - 1 \right] / (\lambda_i + \lambda_j) \end{aligned} \quad (\text{A-11})$$

where $\mathbf{H}(i, j)$ is the (i, j) th entry of \mathbf{H} .

According to (A-11), \mathbf{H} can be deduced as

$$\mathbf{H} = \mathbf{F} \circ \mathbf{J} \quad (\text{A-12})$$

where “ \circ ” is the Hadamard product [58]; and \mathbf{J} is the matrix in which the (i, j) th entry is $[e^{(\lambda_i + \lambda_j)(t-t_0)} - 1]/(\lambda_i + \lambda_j)$.

Substituting \mathbf{H} (A-12) into $\text{Var}[\mathbf{X}(t)]$ (A-9), one obtains the system state covariance as

$$\begin{aligned} \text{Var}[\mathbf{X}(t)] &= \mathbf{P}[\mathbf{F} \circ \mathbf{J}]\mathbf{P}^T \\ &= \mathbf{P} \{ [\mathbf{P}^{-1} \mathbf{K} \mathbf{K}^T (\mathbf{P}^{-1})^T] \circ \mathbf{J} \} \mathbf{P}^T. \quad (\text{A-13}) \end{aligned}$$

ACKNOWLEDGMENT

The authors would like to thank the anonymous editors and reviewers for many helpful corrections and suggestions to improve this paper. The authors also gratefully acknowledge Dr. W. Zhu and Dr. R. Mee for their guidance on this research.

REFERENCES

- [1] S. V. Dhople and A. D. Dominguez-Garcia, “A parametric uncertainty analysis method for Markov reliability and reward models,” *IEEE Trans. Rel.*, vol. 61, no. 3, pp. 634–648, Sep. 2012.
- [2] R. Preece and J. V. Milanović, “Assessing the applicability of uncertainty importance measures for power system studies,” *IEEE Trans. Power Syst.*, vol. 31, no. 3, pp. 2076–2084, May 2016.
- [3] S. V. Dhople, Y. C. Chen, L. De Ville, and A. D. Dominguez-Garcia, “Analysis of power system dynamics subject to stochastic power injections,” *IEEE Trans. Circuits Syst. I, Reg. Papers*, vol. 60, no. 12, pp. 3341–3353, Dec. 2013.
- [4] K. N. Hasan, R. Preece, and J. V. Milanovic, “Priority ranking of critical uncertainties affecting small-disturbance stability using sensitivity analysis techniques,” *IEEE Trans. Power Syst.*, vol. 32, no. 4, pp. 2629–2639, Jul. 2017.
- [5] H. Y. Wu *et al.*, “Stochastic multi-timescale power system operations with variable wind generation,” *IEEE Trans. Power Syst.*, vol. 32, no. 5, pp. 3325–3337, Sep. 2017.
- [6] C. Zhang and J. H. Wang, “Optimal transmission switching considering probabilistic reliability,” *IEEE Trans. Power Syst.*, vol. 29, no. 2, pp. 974–975, Mar. 2014.
- [7] Y. L. Liu and Y. X. Yu, “Probabilistic steady-state and dynamic security assessment of power transmission system,” *Sci. China-Technol. Sci.*, vol. 56, no. 5, pp. 1198–1207, May 2013.
- [8] S. C. Liu, X. Y. Wang, and P. X. Liu, “A stochastic stability enhancement method of grid-connected distributed energy storage systems,” *IEEE Trans. Smart Grid*, vol. 8, no. 5, pp. 2062–2070, Sep. 2017.
- [9] S. Y. Derakhshandeh, A. S. Masoum, S. Deilami, M. A. S. Masoum, and M. E. H. Golshan, “Coordination of generation scheduling with PEVS charging in industrial microgrids,” *IEEE Trans. Power Syst.*, vol. 28, no. 3, pp. 3451–3461, Aug. 2013.
- [10] A. S. Masoum, S. Deilami, A. Abu-Siada, and M. A. S. Masoum, “Fuzzy approach for online coordination of plug-in electric vehicle charging in smart grid,” *IEEE Trans. Sustain. Energy*, vol. 6, no. 3, pp. 1112–1121, Jul. 2015.
- [11] L. Xie *et al.*, “Wind integration in power systems: Operational challenges and possible solutions,” *Proc. IEEE*, vol. 99, no. 1, pp. 214–232, Jan. 2011.
- [12] S. F. Shen *et al.*, “An adaptive protection scheme for distribution systems with DGs based on optimized thevenin equivalent parameters estimation,” *IEEE Trans. Power Del.*, vol. 32, no. 1, pp. 411–419, Feb. 2017.
- [13] J. Pegueroles-Queralt, F. D. Bianchi, and O. Gomis-Bellmunt, “A power smoothing system based on supercapacitors for renewable distributed generation,” *IEEE Trans. Ind. Electron.*, vol. 62, no. 1, pp. 343–350, Jan. 2015.
- [14] D. Apostolopoulou, A. D. Domínguez-García, and P. W. Sauer, “An assessment of the impact of uncertainty on automatic generation control systems,” *IEEE Trans. Power Syst.*, vol. 31, no. 4, pp. 2657–2665, Jul. 2016.
- [15] P. Ferraro, E. Crisostomi, M. Raugi, and F. Milano, “Analysis of the impact of microgrid penetration on power system dynamics,” *IEEE Trans. Power Syst.*, vol. 32, no. 5, pp. 4101–4109, Sep. 2017.
- [16] P. M. Anderson, and M. Mirheydar, “A low-order system frequency response model,” *IEEE Trans. Power Syst.*, vol. 5, no. 3, pp. 720–729, Aug. 1990.
- [17] H. Ye, W. Pei, and Z. P. Qi, “Analytical modeling of inertial and droop responses from a wind farm for short-term frequency regulation in power systems,” *IEEE Trans. Power Syst.*, vol. 31, no. 5, pp. 3414–3423, Sep. 2016.
- [18] Y. F. Mu, J. Z. Wu, J. Ekanayake, N. Jenkins, and H. J. Jia, “Primary frequency response from electric vehicles in the Great Britain Power System,” *IEEE Trans. Smart Grid*, vol. 4, no. 2, pp. 1142–1150, Jun. 2013.
- [19] G. Benysek, J. Bojarski, R. Smolenski, M. Jarnut, and S. Werminski, “Application of stochastic decentralized active demand response (DADR) system for load frequency control,” *IEEE Trans. Smart Grid*, vol. 9, no. 2, pp. 1055–1062, Mar. 2018.
- [20] P. Babahajiani, Q. Shafiee, and H. Bevrani, “Intelligent demand response contribution in frequency control of multi-area power systems,” *IEEE Trans. Smart Grid*, vol. 9, no. 2, pp. 1282–1291, Mar. 2018.
- [21] D. L. H. Aik, “A general-order system frequency response model incorporating load shedding: Analytic modeling and applications,” *IEEE Trans. Power Syst.*, vol. 21, no. 2, pp. 709–717, May 2006.
- [22] R. F. Yan and T. K. Saha, “Frequency response estimation method for high wind penetration considering wind turbine frequency support functions,” *IET Renewable Power Gener.*, vol. 9, no. 7, pp. 775–782, Sep. 2015.
- [23] D. Ochoa and S. Martinez, “Fast-frequency response provided by df-g-wind turbines and its impact on the grid,” *IEEE Trans. Power Syst.*, vol. 32, no. 5, pp. 4002–4011, Sep. 2017.
- [24] H. Huang and F. Li, “Sensitivity analysis of load-damping characteristic in power system frequency regulation,” *IEEE Trans. Power Syst.*, vol. 28, no. 2, pp. 1324–1335, May 2013.
- [25] T. Shekari, F. Aminifar, and M. Sanaye-Pasand, “An analytical adaptive load shedding scheme against severe combinational disturbances,” *IEEE Trans. Power Syst.*, vol. 31, no. 5, pp. 4135–4143, Sep. 2016.
- [26] S. Y. Liao *et al.*, “Load-damping characteristic control method in an isolated power system with industrial voltage-sensitive load,” *IEEE Trans. Power Syst.*, vol. 31, no. 2, pp. 1118–1128, Mar. 2016.
- [27] J. B. Hu, L. Sun, X. M. Yuan, S. Wang, and Y. N. Chi, “Modeling of type 3 wind turbines with df/dt inertia control for system frequency response study,” *IEEE Trans. Power Syst.*, vol. 32, no. 4, pp. 2799–2809, Jul. 2017.
- [28] H. Ahmadi and H. Ghasemi, “Security-constrained unit commitment with linearized system frequency limit constraints,” *IEEE Trans. Power Syst.*, vol. 29, no. 4, pp. 1536–1545, Jul. 2014.
- [29] C. Pradhan and C. N. Bhende, “Frequency sensitivity analysis of load damping coefficient in wind farm-integrated power system,” *IEEE Trans. Power Syst.*, vol. 32, no. 2, pp. 1016–1029, Mar. 2017.
- [30] T. Odun-Ayo and M. L. Crow, “Structure-preserved power system transient stability using stochastic energy functions,” *IEEE Trans. Power Syst.*, vol. 27, no. 3, pp. 1450–1458, Aug. 2012.
- [31] Z. Y. Dong, J. H. Zhao, and D. J. Hill, “Numerical simulation for stochastic transient stability assessment,” *IEEE Trans. Power Syst.*, vol. 27, no. 4, pp. 1741–1749, Nov. 2012.
- [32] K. Wang and M. L. Crow, “The Fokker–Planck equation for power system stability probability density function evolution,” *IEEE Trans. Power Syst.*, vol. 28, no. 3, pp. 2994–3001, Aug. 2013.
- [33] P. Ju, H. Li, C. Gan, Y. Liu, Y. Yu, and Y. Liu, “Analytical assessment for transient stability under stochastic continuous disturbances,” *IEEE Trans. Power Syst.*, vol. 33, no. 2, pp. 2004–2014, Mar. 2018.
- [34] X. Cao, B. Stephen, I. F. Abdulhadi, C. D. Booth, and G. M. Burt, “Switching Markov Gaussian models for dynamic power system inertia estimation,” *IEEE Trans. Power Syst.*, vol. 31, no. 5, pp. 3394–3403, Sep. 2016.
- [35] Y. C. Chen and A. D. Dominguez-Garcia, “A method to study the effect of renewable resource variability on power system dynamics,” *IEEE Trans. Power Syst.*, vol. 27, no. 4, pp. 1978–1989, Nov. 2012.
- [36] J. Ma, Z. X. Song, Y. X. Zhang, Y. Zhao, and J. S. Thorp, “Robust stochastic stability analysis method of DFIG integration on power system considering virtual inertia control,” *IEEE Trans. Power Syst.*, vol. 32, no. 5, pp. 4069–4079, Sep. 2017.
- [37] M. Perninge and L. Soder, “A stochastic control approach to manage operational risk in power systems,” *IEEE Trans. Power Syst.*, vol. 27, no. 2, pp. 1021–1031, May 2012.
- [38] J. C. Pidre, C. J. Carrillo, and A. E. F. Lorenzo, “Probabilistic model for mechanical power fluctuations in asynchronous wind parks,” *IEEE Trans. Power Syst.*, vol. 18, no. 2, pp. 761–768, May 2003.
- [39] K. Hua, Y. Mishra, and G. Ledwich, “Fast unscented transformation-based transient stability margin estimation incorporating uncertainty of wind generation,” *IEEE Trans. Sustain. Energy*, vol. 6, no. 4, pp. 1254–1262, Oct. 2015.

- [40] H. Li, P. Ju, C. Gan, F. Wu, Y. Zhou, and Z. Dong, "Stochastic stability analysis of the power system with losses," *Energies*, vol. 11, no. 3, 2018, Art. no. 678.
- [41] P. Ju, H. Li, X. Pan, C. Gan, Y. Liu, and Y. Liu, "Stochastic dynamic analysis for power systems under uncertain variability," *IEEE Trans. Power Syst.*, vol. 33, no. 4, pp. 3789–3799, Jul. 2018.
- [42] F. Milano and R. Zárate-Miñano, "A systematic method to model power systems as stochastic differential algebraic equations," *IEEE Trans. Power Syst.*, vol. 28, no. 4, pp. 4537–4544, Nov. 2013.
- [43] G. Ghanavati, P. D. H. Hines, and T. I. Lakoba, "Identifying useful statistical indicators of proximity to instability in stochastic power systems," *IEEE Trans. Power Syst.*, vol. 31, no. 2, pp. 1360–1368, Mar. 2016.
- [44] B. Yuan, M. Zhou, G. Li, and X. P. Zhang, "Stochastic small-signal stability of power systems with wind power generation," *IEEE Trans. Power Syst.*, vol. 30, no. 4, pp. 1680–1689, Jul. 2015.
- [45] J. Y. Zhang, P. Ju, Y. P. Yu, and F. Wu, "Responses and stability of power system under small gauss type random excitation," *Sci. China-Technol. Sci.*, vol. 55, no. 7, pp. 1873–1880, Jul. 2012.
- [46] C. O. Nwankpa and S. M. Shahidehpour, "Stochastic model for power system planning studies," *IEE Proc. C-Gener. Transmiss. Distrib.*, vol. 138, no. 4, pp. 307–320, 1991.
- [47] H. Mohammed and C. O. Nwankpa, "Stochastic analysis and simulation of grid-connected wind energy conversion system," *IEEE Trans. Energy Convers.*, vol. 15, no. 1, pp. 85–90, Mar. 2000.
- [48] X. Wang, H. D. Chiang, J. Wang, H. Liu, and T. Wang, "Long-term stability analysis of power systems with wind power based on stochastic differential equations: Model development and foundations," *IEEE Trans. Sustain. Energy*, vol. 6, no. 4, pp. 1534–1542, Oct. 2015.
- [49] R. Zarate-Minano, M. Anghel, and F. Milano, "Continuous wind speed models based on stochastic differential equations," *Appl. Energy*, vol. 104, pp. 42–49, Apr. 2013.
- [50] F. P. D. Mello, "Boiler models for system dynamic performance studies," *IEEE Trans. Power Syst.*, vol. 6, no. 1, pp. 66–74, Feb. 1991.
- [51] F. P. Demello, "Dynamic-models for fossil fueled steam units in power-system studies," *IEEE Trans. Power Syst.*, vol. 6, no. 2, pp. 753–761, May 1991.
- [52] T. Inoue, H. Taniguchi, and Y. Ikeguchi, "A model of fossil fueled plant with once-through boiler for power system frequency simulation studies," *IEEE Trans. Power Syst.*, vol. 15, no. 4, pp. 1322–1328, Nov. 2000.
- [53] F. P. Demello *et al.*, "Hydraulic-turbine and turbine control-models for system dynamic studies," *IEEE Trans. Power Syst.*, vol. 7, no. 1, pp. 167–179, Feb. 1992.
- [54] S. K. Yee, J. V. Milanovic, and F. M. Hughes, "Overview and comparative analysis of gas turbine models for system stability studies," *IEEE Trans. Power Syst.*, vol. 23, no. 1, pp. 108–118, Feb. 2008.
- [55] J. J. Dai, D. Xiao, F. Shokooch, C. Schaeffer, and A. Benge, "Emergency generator startup study of a hydro turbine unit for a nuclear generation facility," *IEEE Trans. Ind. Appl.*, vol. 40, no. 5, pp. 1191–1199, Sep/Oct. 2004.
- [56] D. Hill and A. Bergen, "Stability analysis of multimachine power networks with linear frequency dependent loads," *IEEE Trans. Circuits Syst.*, vol. 29, no. 12, pp. 840–848, Dec. 1982.
- [57] X. Mao, *Stochastic Differential Equations and Applications*. Amsterdam, The Netherlands: Elsevier, 2007.
- [58] R. A. Horn, and C. R. Johnson, *Matrix Analysis*. Cambridge, U.K.: Cambridge Univ. Press, 1990.
- [59] J. Qui, S. M. Shahidehpour, and Z. Schuss, "Effect of small random perturbations on power systems dynamics and its reliability evaluation," *IEEE Trans. Power Syst.*, vol. 4, no. 1, pp. 197–204, Feb. 1989.
- [60] Iceland network dynamic data. [Online]. Available: <http://www.maths.ed.ac.uk/optenergy/NetworkData/icelandDyn/>
- [61] Y. Chompoobutgool, W. Li, and L. Vanfretti, "Development and implementation of a Nordic grid model for power system small-signal and transient stability studies in a free and open source software," in *Proc. IEEE Power Energy Soc. Gen. Meet.*, 2012, pp. 1–8.



Hongyu Li (S'14) received the B.S. degree in electrical engineering, in 2012. He is currently working toward the Ph.D. degree in electrical engineering at Hohai University, Nanjing, China. He is currently performing research with the University of Tennessee, Knoxville, TN, USA, as a Visiting Student. His research interests include power system dynamic analysis under stochastic disturbances.



Ping Ju (M'95–SM'10) received the B.S. and M.S. degrees from Southeast University, Nanjing, China, in 1982 and 1985, respectively, and the Ph.D. degree from Zhejiang University, Hangzhou, China, all in electrical engineering. He is currently a Professor of electrical engineering with Hohai University, Nanjing, China and Zhejiang University, Hangzhou, China. From 1994 to 1995, he was an Alexander-von Humboldt Fellow with the University of Dortmund, Germany.

His research interests include modeling and control of power system with integration of renewable generation.

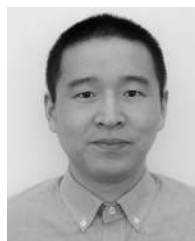


Chun Gan (M'14) received the Ph.D. degree in electrical engineering and motor drives from Zhejiang University, Hangzhou, China, in 2016.

He is currently with the School of Electrical and Electronic Engineering, Huazhong University of Science and Technology, Wuhan, China. From September 2016 to September 2018, he was a Research Associate with the Department of Electrical Engineering and Computer Science, University of Tennessee, Knoxville, TN, USA. He has authored/coauthored more than 60 peer-reviewed technical papers. He has 12 issued/published invention patents. His research interests include electrical motor drives, electric vehicles, high-efficiency power converters, and microgrid.

Dr. Gan was the recipient of the 2018 Highlighted Paper Award from IEEE TRANSACTIONS ON POWER ELECTRONICS, the 2018 Marie Skłodowska-Curie Actions Seal of Excellence Award from European Commission, the 2016 Excellent Ph.D. Graduate Award, the 2015 Top Ten Excellent Scholar Award, and the 2015 National Scholarship in Zhejiang University.

Dr. Gan was the recipient of the 2018 Highlighted Paper Award from IEEE TRANSACTIONS ON POWER ELECTRONICS, the 2018 Marie Skłodowska-Curie Actions Seal of Excellence Award from European Commission, the 2016 Excellent Ph.D. Graduate Award, the 2015 Top Ten Excellent Scholar Award, and the 2015 National Scholarship in Zhejiang University.



Shutang You (S'13) received the B.S. and M.S. degrees from Xi'an Jiaotong University, Xi'an, China, in 2011 and 2014, respectively, and the Ph.D. degree in electrical engineering from the University of Tennessee, Knoxville, TN, USA, in 2017. He is currently a Research Assistant Professor with the Department of Electrical Engineering and Computer Science, University of Tennessee, Knoxville, TN, USA.

His research interests include power grid dynamics and monitoring.



Feng Wu received the B.Eng. and M.Sc. degrees in electrical engineering from Hohai University, Nanjing, China, in 1998 and 2002, respectively, and the Ph.D. degree in electrical engineering from the University of Birmingham, Birmingham, U.K., in 2009. He is currently a Professor with Hohai University, Nanjing, China.

His research interests include modeling and control of the renewable energy generation.



Yilu Liu (S'88–M'89–SM'99–F'04) received the the B.S. degree from Xi'an Jiaotong University, Xi'an, China, and the M.S. and Ph.D. degrees from the Ohio State University, Columbus, OH, USA, in 1986 and 1989, respectively.

Prior to joining UTK/ORNL, she was a Professor with Virginia Tech, Blacksburg, VA, USA. She led the effort to create the North American Power Grid Frequency Monitoring Network at Virginia Tech, which is now operated at UTK and ORNL as GridEye. Her research interests include power system wide-area

monitoring and control, large interconnection-level dynamic simulations, electromagnetic transient analysis, and power transformer modeling and diagnosis.

Dr. Liu is currently the Governor's Chair with the University of Tennessee, Knoxville, TN, USA, and Oak Ridge National Laboratory (ORNL). She is elected as the Member of National Academy of Engineering, in 2016. She is also the Deputy Director of the DOE/NSFcofunded Engineering Research Center CURENT.